# Semidiurnal Dynamics of Salinity, Nutrients and Suspended Particulate Matter in an Estuary in the Seto Inland Sea, Japan, during a Spring Tide Cycle

PAOLO MAGNI[†], SHIGERU MONTANI* and KUNINAO TADA

*Department of Life Sciences, Faculty of Agriculture, Kagawa University,*
*Miki, Kagawa 761-0795, Japan*

The physical and chemical variability of the water column at subtidal station of an estuary in the Seto Inland Sea, Japan, was studied over a 24-hour period during a spring tide (tidal range *ca.* 2 m) in May 1995. Surface water and several depths through the water column were monitored every one and two hours, respectively. At each occasion, water temperature, salinity and dissolved oxygen concentration were measured and water samples were collected for the determination of nutrients and suspended particulate matter (SPM). Disruptive changes in the physical and chemical characteristics of the water was produced by the tidal cycle and the mixing of water masses of different origin. These changes were highly significant both spatially and temporally, yet with varying effects on physical parameters, nutrients and the different components of SPM. Significant differences in nutrient concentrations were also observed when the data-set was divided into ebb and flood components, irrespective of the depth. Nitrate and nitrite rose to 1.8 times higher during the flood. Spatial differences of SPM were less marked than those of nutrients, only particulate organic carbon (POC) being significantly higher at the surface than in the intermediate and the lower layer. Both POC and pheopigment concentrations increased markedly through the water column, being highest shortly before the lower low tide. In contrast, suspended solid (SS) content increased sharply after the lower low tide (>40 mg $l^{-1}$) and this coincided with a marked decrease of the C/SS content (<20 mg $g^{-1}$). The lagtime between POC and SS tidal transport was caused by particle resuspension from the exposed intertidal sediments as the tidal level rose, and particle transport selection in relation to the tidal state.

## 1. Introduction

A fundamental aspect in the study of the dynamics of biophilic elements (i.e. carbon, nitrogen, phosphorus and silicon) in tidal estuaries relates to the short-term variability of the water chemistry, which is strongly influenced by the effect of a tidal cycle. On a time-scale of hours, ebb advection of fresh water and salt water intrusion during the flood can be responsible for major changes in salinity (Yin *et al.*, 1995a; Uncles and Stephens, 1996; Montani *et al.*, 1998), nutrient concentrations (Caffrey and Day, 1986; Hernandez-Ayon *et al.*, 1993; Montani *et al.*, 1998) and suspended solid content (Caffrey and Day, 1986; Renshun, 1992). The extent of such changes will further vary depending on spring-neap tidal state or amplitude (Vörösmarty and Loder, 1994; Yin *et al.*, 1995b; Uncles and Stephens, 1996), current velocity (Renshun, 1992; Dyer *et al.*, 2000), winds (Yin *et al.*, 1995c; Dyer *et al.*, 2000) and precipitation rate, which affects fresh water discharge (Schubel and Pritchard, 1986; Page *et al.*, 1995).

In several time series surveys, plots of nutrients as a function of salinity have been used as a valuable tool to assess the different sources of nutrients species, whether from inland, outside the estuary or within it (Balls, 1992, 1994; Clark *et al.*, 1992; Page *et al.*, 1995; Eyre and Twigg, 1997; Montani *et al.*, 1998). Other works have focused on the seasonal change in the concentration of

* Corresponding author. E-mail: montani@ag.kagawa-u.ac.jp

[†] Present address: International Marine Centre, Coastal Ecosystems Group, Localita' Sa Mardini 09072 Torregrande - Oristano, Italy.

nutrients and/or particulate compounds (Caffrey and Day, 1986; Ward and Twilley, 1986; Cowan et al., 1996; Bianchi and Argyrou, 1997), or the temporal variation of river discharge as a major source of microalgal materials to estauries (Bennett et al., 1986; Murakami et al., 1992, 1994; De Madariaga, 1995), terrestrial organic matter (Bianchi and Argyrou, 1997) or suspended solids (Caffrey and Day, 1986; Schubel and Pritchard, 1986). However, no detailed information can be found in the published literature on the short-term spatial and temporal (24-h) variability of both dissolved (nutrients) and particulate (SPM) compounds (i.e. Chlorophyll a, pheopigments, organic carbon and suspended solids), on an hourly basis over a complete tidal cycle. The distributional pattern and behaviour among various compounds is likely to vary both in quality and quantity, given their different nature, and the variation would be independent of seasonal patterns. In particular, this may be closely related to the extent of low salinity water mass intrusion, the differentiated export of nutrients and SPM, and possible resuspension and transport of living and/or non-living particles from the bottom sediments produced by the tidal cycle and yet depending on the tidal state (i.e. low tide vs. high tide) and amplitude (i.e. lower vs. higher low and high tides).

We carried out this study in the context of a long-term interdisciplinary project which aims to quantify the cycling of biophilic elements in a tidal estuary of the Seto Inland Sea, Japan (Magni, 1998; Montani et al., 1998; Magni and Montani, 2000), and to assess the role played by primary producers (Magni and Montani, 1997; Magni et al., 2000a) and consumers (Magni and Montani, 1998; Magni et al., 2000b) in this cycling. In the present study, our first objective was to investigate the tidally-mediated spatial variability of temperature, salinity, and dissolved oxygen (D.O.) and nutrient concentrations through the water column over a complete tidal cycle. This study is integrated with complementary work that we conducted simultaneously on the horizontal distribution of these parameters in surface water along the estuary (Montani et al., 1998). We here extend the investigations to major components of SPM (i.e. Chlorophyll a, pheopigments, particulate organic carbon and suspended solids), together with temperature, salinity, D.O. and nutrients, on a seasonal basis (Magni and Montani, 2000). Secondly, we aimed to investigate and assess the temporal variability of both physical and chemical parameters over a 24-h period, in particular qualitative and quantitative differences between a high tide and a low tide situation. Since this is a mixed-semidiurnal type estuary (with pronounced differences between two successive low and high tides), we also aimed to evaluate the influence of the tidal amplitude on the variability of the water chemistry. We also discuss spatial and temporal differences in distributional patterns between dissolved and particulate compounds and

the ecological relevance of the tidal export to the subtidal benthic environment and macrofaunal communities also investigated at this station (Magni and Montani, 1998).

## 2. Materials and Methods

### 2.1 Study area and sampling

We conducted the time series experiments at an innermost station (Stn. Y3) in the subtidal zone of an estuary of the Seto Inland Sea (Fig. 1), during a spring tide of May 1995. This station, with a depth of ca. 10 m at high tide, has also been the focus of previous, associated work on the short-term (Montani et al., 1998) and seasonal (Magni and Montani, 2000) variability of surface water,
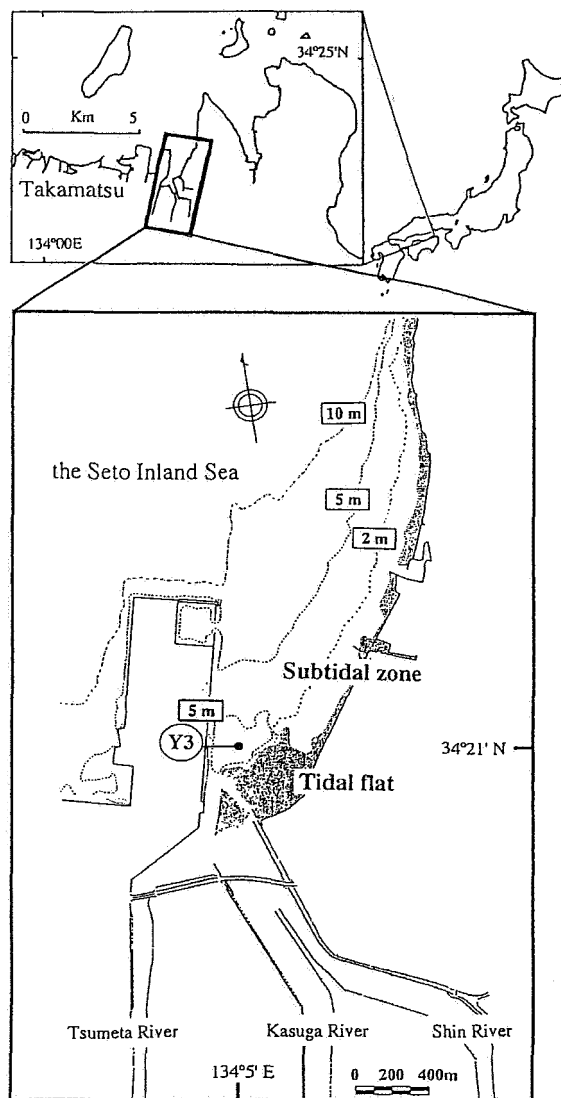


Fig. 1. Study area and location of the sampling station (Stn. Y3) at an innnermost site of the subtidal zone.

and on the seasonal changes of major chemical parameters in surface sediments (phytopigments, total organic carbon and acid volatile sulfides) and macrofaunal communities (Magni and Montani, 1998).

The survey of the present study started at 10:00 on the 30th and ended at 10:00 on the next day. Two lower and two higher tidal levels were predicted during the sampling period (Maritime Safety Agency, Takamatsu). The first high tide, at 10:57, was +197 cm and the second one, at 0:24, was +239 cm. We used the difference in tidal height to distinguish them as a lower and a higher high tide, respectively. Correspondingly, a lower low tide at 17:28 and a higher low tide at 6:41 occurred, which were +35 cm and +105 cm, respectively. The largest difference of the tidal level was 204 cm, between 17:28 and 0:24. During the survey the weather was fine, following two days of little rain (Montani et al., 1998). We can therefore assume that the strength of river runoff was not influenced during the course of the survey by variations in rainfall, which would rapidly affect salinity in our study area (Magni and Montani, 2000). Every hour, hydrological measurements (salinity, measured using the Practical Salinity Scale, temperature and dissolved oxygen) were made at 1 m intervals from the surface to the bottom, using a CTD cast (Alec ADO 1050-D), and surface water was collected using a clean bucket. Every other hour, water samples were collected from four additional depths through the water column using 6-1 Van Dorn bottles. These layers included 1, 3, and 5 m layers and the 1–2 m layer above the bottom. At 4:00 and 6:00 we could also collect from the surface and at three other depths, giving a total of 75 samples. At each sampling occasion the water samples were transferred into 5-1 polyethylene bags and stored on the boat in the dark at the in situ water temperature.

## 2.2 Sample treatment and analysis

Every six hours the water samples were brought to the laboratory for further treatment and later determination of nutrients [$NH_4^+$-N, ($NO_3^-$+$NO_2^-$)-N, $PO_4^{3-}$-P and Si(OH)$_4$-Si] and suspended particulate matter (SPM: Chlorophyll $a$, pheopigments, particulate organic carbon and suspended solids). For the analysis of nutrients, subsamples were filtered through Nucleopore filters (0.4 $\mu$m pore size) and concentrations were determined in duplicate with a Technicon autoanalyzer II, according to Strickland and Parsons (1972). For the analysis of Chlorophyll $a$ (Chl $a$) and pheopigments, 0.5 to 1 l of water was filtered through Whatman GF/F glass fiber filters. Pigments were extracted using a 90% acetone solution. After 24 h extraction in the dark at 4°C, Chl $a$ and pheopigments were spectrophotometrically analyzed according to Lorenzen's (1967) method, as described by Parsons et al. (1984). For the analysis of particulate or-

ganic carbon (POC) and the determination of suspended solids (SS), the same volume of water used for pigment analysis was filtered through pre-ignited (450°C for 2 h) and pre-weighed Whatman GF/F filters. These filters were washed with distilled water to remove salts. They were stored at –20°C, and later freeze-dried and weighed for the determination of SS. The samples were pre-treated with 12 N HCl vapour to remove the carbonates and neutralized with NaOH before analysis for POC, using a CHN analyzer (Yanako MT-3).

ANOVA (Sokal and Rohlf, 1995) was used to analyse the significance of the correlation among the examined parameters, and spatial and temporal differences of the data set.

## 3. Results

### 3.1 Temperature, salinity and dissolved oxygen

Water temperature varied from 16.3°C at 11:00 (7 m and 8 m) to 20.9°C at 17:00 (surface) (Fig. 2(a)). The strongest increase of temperature occurred at the uppermost 2–3 m, during the lower low tide, between 14:00 and 19:00 (Fig. 2(a)). In contrast, soon after the higher high tide, between 1:00 and 3:00, temperature values were homogeneously distributed through the water column, ranging between 16.5°C (lower depths) and 16.8°C (surface). Water temperature progressively increased again during the next higher low tide. However, this increase was more restricted, up to 18.4°C at the surface at 10:00 on May 31.

Salinity was slightly different among layers at the start of the survey, varying from 31.3 (surface) to 32.0 (8 m), but decreased markedly within the next few hours (Fig. 2(b)). A major variation in salinity occurred at the surface, with a minimum of 17.5 at 21:00. At other depths, salinity remained constantly >31.2. From 23:00 to 3:00, salinity was again distributed homogeneously, but was slightly lower at the surface, e.g. <31 between 24:00 and 2:00 (Fig. 2(b)). During the higher low tide, surface salinity decreased again, but to a more limited extent with a minimum of 26.3 at 8:00.

Dissolved oxygen (D.O.) concentration varied between 6.1 mg l$^{-1}$ at 7:00 (surface) and 11.3 mg l$^{-1}$ at 19:00 (1 m) (Fig. 2(c)). A noticeable decrease of D.O. concentration (<8.0 mg l$^{-1}$) occurred at the surface during the two low tides and at lower layers down to the bottom from 17:00 to 3:00 (Fig. 2(c)). From 6:00 to 10:00, D.O. concentration tended to be lower (between 7 mg l$^{-1}$ and 8 mg l$^{-1}$) than that found during the first part of the survey (between 8 mg l$^{-1}$ and 9 mg l$^{-1}$) (Fig. 2(c)).

### 3.2 Nutrients

The spatial and temporal distribution of different nutrient species (ammonium, nitrate + nitrite, phosphate
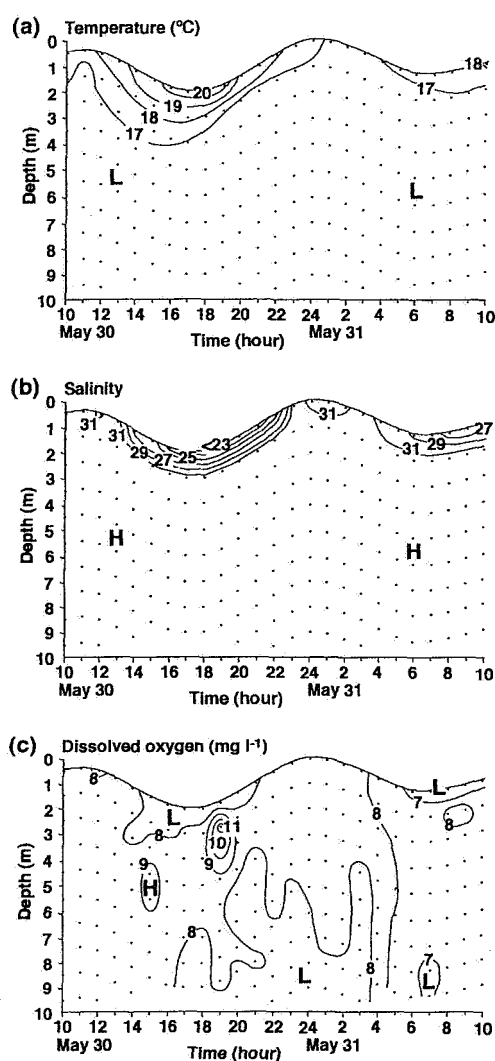
Fig. 2. Time series contours of (a) temperature, (b) salinity and (c) dissolved oxygen (D.O.) concentration.

and silicate) was quite similar between species. Nutrient concentrations changed drastically on a time scale of 1–2 hours, strongly depended on the tidal cycle, and tended to decrease remarkably with depth at each sampling occasion (Figs. 3(a), (b), (c) and (d)).

Ammonium nitrogen ($NH_4^+$-N) concentration varied from 3.7 $\mu$M (3 m, 24:00) to 42.6 $\mu$M (surface, 3:00) (Fig. 3(a)). At the start, ammonium concentration was homogeneously low through the water column, varying between 5 $\mu$M and 10 $\mu$M. At the following hour, an increase >10 $\mu$M occurred at the surface. Such an increase further progressed down to 1 m at 12:00 and included the whole water column at 14:00. As the lower low tide approached, ammonium concentration varied more drastically at the surface, up to 24.6 $\mu$M at 14:00 and 31.9 $\mu$M at 15:00. A subsequent major increase occurred at the surface between

19:00 (35.7 $\mu$M) and 21:00 (34.7 $\mu$M), while ammonium concentration remained constantly ≤15 $\mu$M below the surface, with a minimum of 4.6 $\mu$M at 7 m at 20:00. With the surging flood of the higher high tide, ammonium concentration at the surface dropped rapidly from 19.6 $\mu$M at 22:00 to 4.8 $\mu$M at 23:00. During the higher high tide, ammonium concentration was lowest, with values <7 $\mu$M through the water column. Subsequently, a marked vertical gradient was restored with the coming ebb. Values increased up to >30 $\mu$M between 2:00 and 3:00 at the surface, and were >15 $\mu$M at 1 m at 4:00 and down to 7 m at 8:00. At the end of the time series, at 10:00 on May 31, ammonium concentration tended to decrease again through the water column.

Nitrate + nitrite nitrogen [($NO_3^-$+$NO_2^-$)-N] concentration varied from 2.8 $\mu$M (7 m, 20:00) to 50.3 $\mu$M (surface, 2:00) (Fig. 3(b)), i.e. the range of fluctuation was relatively larger than that of ammonium (Fig. 3(a)). On a total of 75 samples, nitrate + nitrite concentration was ≤5 $\mu$M in 24 occasions, most of them found during the higher high tide period (Fig. 3(b)), while ammonium concentration was ≤5 $\mu$M only in five samples (Fig. 3(a)).

Phosphate concentration ($PO_4^{3-}$-P) varied from 0.54 $\mu$M (3 m, 22:00) to 4.9 $\mu$M (surface, 20:00) (Fig. 3(c)). At the start of the time series, phosphate concentration was <1 $\mu$M at all depths. Similarly to the nitrogen nutrient species, phosphate concentration sharply increased during both low tides, with values >2.0 $\mu$M down to the near-bottom depth at 8:00 on May 31, while it was homogeneously low during the higher high tide, with a minimum of 0.80 ± 0.25 $\mu$M at 24:00.

During the first four hours of the survey, silicate [Si(OH)$_4$-Si] concentration (Fig. 3(d)) remained rather homogeneously low, varying from 10.7 $\mu$M (7.5 m, 10:00) to 14.9 $\mu$M (1 m, 12:00). At 14:00, approaching the lower low tide and with a coincident decrease of surface salinity <29 (Fig. 2(b)), silicate concentration peaked sharply at the surface with 42.5 $\mu$M, while it remained <20 $\mu$M at the other depths. At 16:00, surface silicate concentration increased up to 58.6 $\mu$M. This was also accompanied by a noticeable increase in intermediate layers (26.9 $\mu$M at 1 m and 21.0 $\mu$M at 3 m). However, similarly to the spatial distribution of phosphate concentration, silicate concentration increased further at the surface during the next few hours, up to a maximum of 76.7 $\mu$M at 20:00, while it rapidly decreased at the other depths, with values <20 $\mu$M. During the higher high tide, between 23:00 and 1:00, silicate concentration also decreased markedly at the surface, with values <20 $\mu$M and a minimum mean of 10.8 ± 2.1 $\mu$M at 24:00. The subsequent spatial and temporal distribution of silicate concentration was similar to that of all other nutrient species, with an increase at the surface between 2:00 and 3:00, and a second major peak at 8:00 with values <20 $\mu$M down to 3 m.
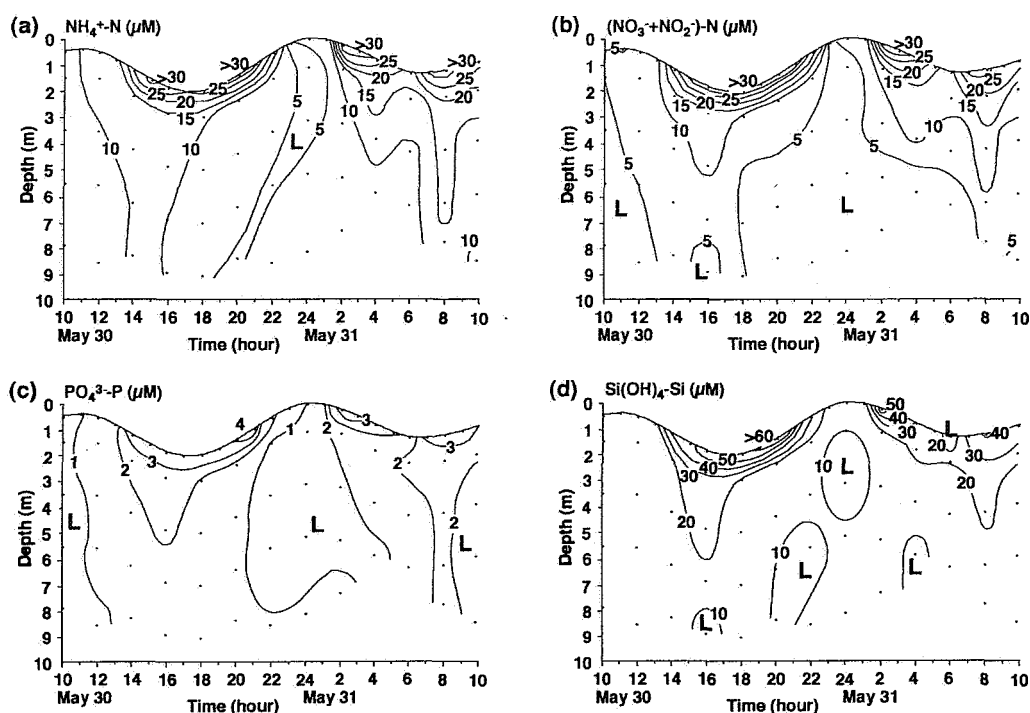
Fig. 3. Time series contours of nutrient concentrations. (a) Ammonium nitrogen ($NH_4^+$-N), (b) nitrate + nitrite nitrogen [($NO_3^-$+$NO_2^-$)-N], (c) phosphate ($PO_4^{3-}$-P) and (d) silicate [$Si(OH)_4$-Si].

### 3.3 Suspended particulate matter (SPM)

In contrast to the behaviour of nutrient species (Figs. 3(a), (b), (c) and (d)), the spatial and temporal distribution of SPM varied remarkably between the component species viz., Chlorophyll a (Chl a), pheopigments, particulate organic carbon (POC) and suspended solid (SS) (Figs. 4(a), (b), (c) and (d)). In addition, the tidal amplitude had a greater impact on most parameters, and the C/Chl a and C/SS ratios (Figs. 4(e) and (f)), than on nutrients. Yet, as for nutrient concentrations, drastic changes occurred on a time scale of 1–2 h.

The Chl a content varied from 1.0 $\mu$g l$^{-1}$ (5 m, 2:00) to 2.9 $\mu$g l$^{-1}$ (surface, 9:00) (Fig. 4(a)). Values ≥2.0 $\mu$g l$^{-1}$ were restricted to the uppermost 3 m, between 18:00 and 21:00 of May 30 and between 7:00 and 10:00 of May 31, but at 16:00 (5 m and 7 m) during the lower low tide. The Chl a concentration decreased to <1.5 $\mu$g l$^{-1}$ at night, with a minimum mean value of 1.2 ± 0.1 $\mu$g l$^{-1}$ at 4:00.

Pheopigments displayed a more marked temporal pattern than Chl a, more noticeably related to the tidal state and amplitude (Fig. 4(b)). During the first three hours of the survey the pheopigment concentration was lower than that of Chl a, varying from 0.3 $\mu$g l$^{-1}$ (surface, 10:00) to 1.0 $\mu$g l$^{-1}$ (7.5 m, 10:00). At 14:00, the pheopigment concentration remained <1 $\mu$g l$^{-1}$ at the surface, but increased markedly at lower depths, up to 2.2 $\mu$g l$^{-1}$ at 3 m.

At 16:00 it increased strongly through out the water column, including the surface, up to the maximum value of 4.7 $\mu$g l$^{-1}$ at 7 m. Subsequently, after the lower low tide, the pheopigment concentration decreased rapidly and at 20:00 it was again lower than that of Chl a. The lowest values occurred at 24:00, with a mean through out the water column of 0.2 ± 0.2 $\mu$g l$^{-1}$. After the higher high tide, a marked increase occurred at the surface between 2:00 (2.4 $\mu$g l$^{-1}$) and 3:00 (2.6 $\mu$g l$^{-1}$), as was also observed for the nutrient concentrations (Figs. 3(a), (b), (c) and (d)). During the higher low tide the pheopigment concentration varied between 1.0 $\mu$g l$^{-1}$ and 2.0 $\mu$g l$^{-1}$. However, such an increase was much more limited than that found during the lower low tide on the previous day. At the end of the survey, the pheopigment concentration was again lower than that of Chl a and <1.0 $\mu$g l$^{-1}$, as it was at the start.

The temporal distribution of POC (Fig. 4(c)) resembled that of pheopigments (Fig. 4(b)). The POC concentration was homogeneously low during the first three hours of the survey, varying from 0.25 mg l$^{-1}$ (3 m, 10:00) to 0.37 mg l$^{-1}$ (7.5 m, 10:00) (Fig. 4(c)). Subsequently, as for pheopigments, POC increased noticeably below the surface at 14:00 with the strongest increase at 16:00, resulting in a maximum value of 1.49 mg l$^{-1}$ at 7 m. After the lower low tide, POC decreased markedly to a mini-
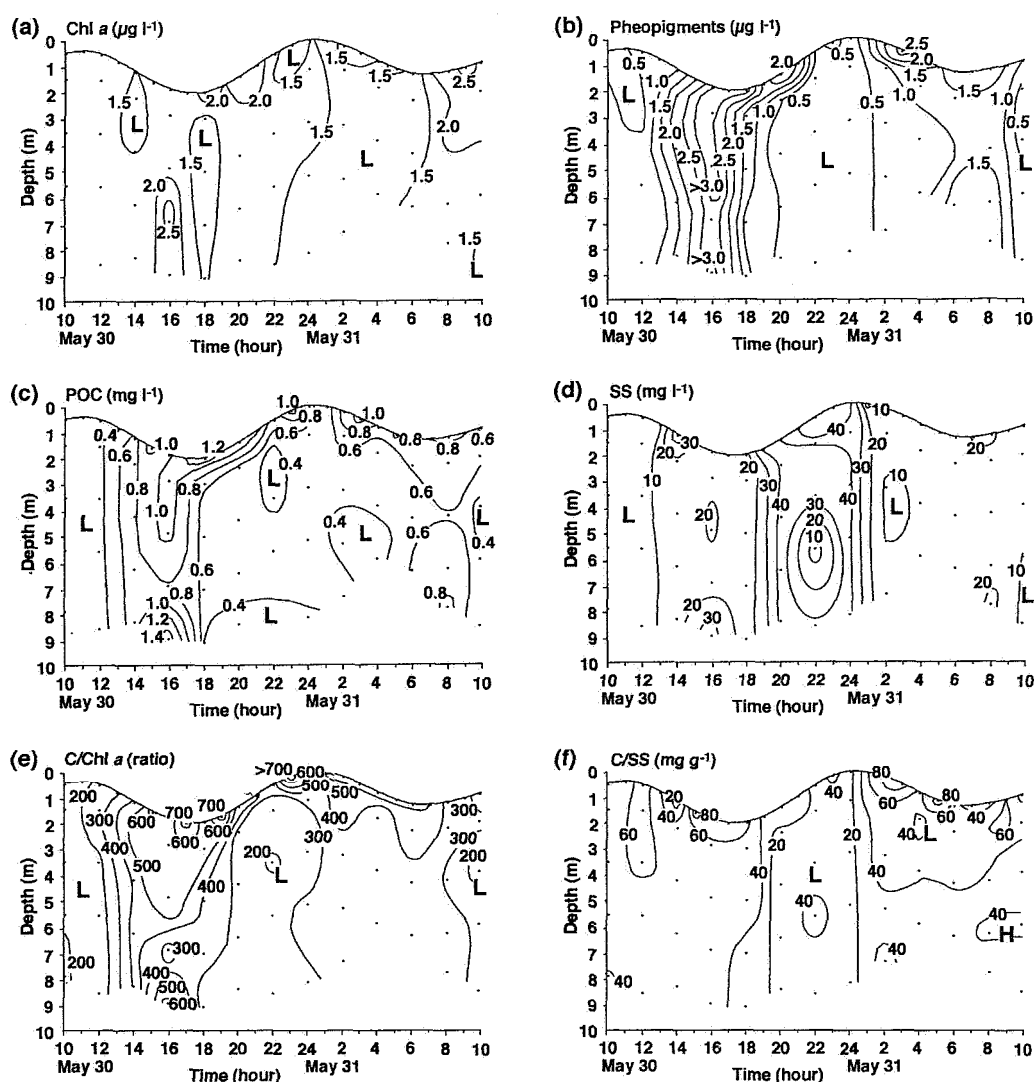
Fig. 4. Time series contours of the examined components of suspended particulate matter (SPM). (a) Chlorophyll *a* (Chl *a*), (b) pheopigments, (c) particulate organic carbon (POC), (d) suspended solids (SS), (e) POC/Chl *a* ratio (C/Chl *a*), (f) POC content in SS (C/SS).

mum mean of $0.46 \pm 0.09$ mg $l^{-1}$ at 24:00. After the higher high tide, a significant increase of POC concentration occurred at the surface between 2:00 (0.99 mg $l^{-1}$) and 3:00 (1.23 mg $l^{-1}$), as found for pheopigments. At the end of the survey, the POC concentration decreased once again to lower values.

Similar to POC, the SS concentration was homogeneously low during the first three hours of the survey with a minimum value of 4.4 mg $l^{-1}$ at 3 m (10:00) (Fig. 4(d)). It increased from 14:00 to 18:00, but to a lesser extent than the increase of pheopigments (Fig. 4(b)) and POC (Fig. 4(c)). The SS concentration tended to fall in between the values 10 mg $l^{-1}$ and 20 mg $l^{-1}$, but was 38.8 mg $l^{-1}$ at the surface (14:00) and 31.9 mg $l^{-1}$ at 7 m (16:00). Be-

tween 18:00 and 20:00, starting with the surging flood of the higher high tide, SS increased drastically from <20 mg $l^{-1}$ to *ca.* 40 mg $l^{-1}$. Between 20:00 and 24:00 values were highest, ranging typically around 40 mg $l^{-1}$ and up to 45.4 mg $l^{-1}$ at the surface at 22:00. During this sampling occasion we also found a low SS concentration (16.7 mg $l^{-1}$) at an intermediate layer (5 m).

The C/Chl *a* ratio was lower than 200 at the start, with a minimum of 143 at 1 m (10:00) (Fig. 4(e)). Within the next few hours this ratio increased strongly to >400 throughout the water column, up to 721 (17:00) and 759 (19:00) at the surface. The C/Chl *a* ratio tended to be higher at the surface than at other depths. A noticeable exception occurred at 16:00, with a high value (695) at 7

m, which related to the highest POC content found during the time series (Fig. 4(c)). From 20:00, at the flood, the C/Chl $a$ ratio decreased markedly below the surface (<300), but remained high at the surface, up to the highest peak of 807 at 23:00. Approaching the next ebb, the C/Chl $a$ ratio increased again through the water column. In contrast to the increase which occurred during the ebb on the previous day (toward the lower low tide), the C/Chl $a$ ratio was >500 only at the surface. As found for pheopigments and POC (Figs. 4(b) and (c)), the increase of the C/Chl $a$ ratio was stronger during the lower low tide, on May 30, than during the higher low tide, on May 31 (Fig. 4(e)).

The temporal pattern of the POC fraction in SS (C/SS = mg g$^{-1}$) (Fig. 4(f)) contrasted with that of SS content (Fig. 4(d)). The C/SS content was high from 10:00 to 18:00 and generally lay between 40 mg g$^{-1}$ and 60 mg g$^{-1}$. During this period, however, the surface was much more variable, ranging between 17.1 mg g$^{-1}$ (14:00) and 81.3 mg g$^{-1}$ (15:00). A drastic decrease of the C/SS content occurred soon after the lower low tide, with a progressive decrease from 40 mg g$^{-1}$ (18:00, 5 and 6 m) to 20 mg g$^{-1}$ (20:00, surface excluded) and a minimum of 7.7 mg g$^{-1}$ at 22:00 (1 m). This pattern was opposite to that of SS, which increased sharply during the same period (Fig. 4(d)). After the higher high tide, the C/SS content increased strongly again, while SS decreased strongly, reaching a maximum at the surface of 88.7 mg g$^{-1}$ (2:00).

### 3.4 Correlation analysis of physical and chemical parameters

Temperature and salinity were highly correlated ($P < 0.001$) with each other, while D.O. was not significantly correlated with either (Table 1). Both temperature and salinity were highly correlated ($P < 0.001$) with all nutrient species. The relevant best-fit regression lines had $R^2$ values varying from 0.36 (temperature) and −0.49 (salinity), for ammonium, to 0.59 and −0.74, respectively, for silicate. Temperature and salinity also showed a positive and a negative correlation, respectively, with the various components of SPM and the examined ratios, but SS (temperature) and C/SS (salinity). However, this correlation was highly significant only for pheopigments, POC and C/Chl $a$ ratio, albeit with fairly low $R^2$ values (Table 1). D.O. was also significantly correlated with all nutrients species, Chl $a$, pheopigments and POC, but with fairly low $R^2$ values. Among the different nutrient species, nitrate + nitrite and silicate showed the strongest correlation with each other ($R^2 = 0.93$, $P < 0.001$). Among SPM components, the strongest correlation was that between pheopigments and POC ($R^2 = 0.62$, $P < 0.001$), while SS was not significantly correlated with either Chl $a$ and pheopigments, or POC (Table 1).

Table 1. Results of product-moment correlation analysis ($R^2$) for the investigated physical and chemical variables (ANOVA, ns: not significant, *: $P < 0.05$, **: $P < 0.01$, ***: $P < 0.001$). Bold values indicate a negative correlation.

| Parameter | Temp. | Salin. | D.O. | NH$_4^+$ | NO$_3^-$-NO$_2^-$ | PO$_4^{3-}$ | Si(OH)$_4$ | Chl $a$ | Pheop. | POC | SS | C/Chl $a$ | C/SS |
|---|---|---|---|---|---|---|---|---|---|---|---|---|---|
| Temp. | 1.00 | | | | | | | | | | | | |
| Salin. | **−0.70***  | 1.00 | | | | | | | | | | | |
| D.O. | ns | ns | 1.00 | | | | | | | | | | |
| NH$_4^+$ | 0.36*** | **−0.49*** | **−0.25*** | 1.00 | | | | | | | | | |
| NO$_3^-$-NO$_2^-$ | 0.45*** | **−0.60*** | **−0.12*** | 0.89*** | 1.00 | | | | | | | | |
| PO$_4^{3-}$ | 0.50*** | **−0.57*** | **−0.23*** | 0.90*** | 0.86*** | 1.00 | | | | | | | |
| Si(OH)$_4$ | 0.59*** | **−0.74*** | **−0.13*** | 0.87*** | 0.93*** | 0.87*** | 1.00 | | | | | | |
| Chl $a$ | 0.05* | **−0.12*** | **−0.08*** | 0.19*** | 0.16*** | 0.21*** | 0.19*** | 1.00 | | | | | |
| Pheop. | 0.17*** | **−0.16*** | **−0.12*** | 0.28*** | 0.24*** | 0.32*** | 0.28*** | 0.12** | 1.00 | | | | |
| POC | 0.36*** | **−0.38*** | **−0.07*** | 0.42*** | 0.47*** | 0.53*** | 0.49*** | 0.17*** | 0.62*** | 1.00 | | | |
| SS | ns | **−0.06*** | ns | ns | ns | ns | ns | ns | ns | ns | 1.00 | | |
| C/Chl $a$ | 0.22*** | **−0.20*** | ns | 0.21*** | 0.25*** | 0.28*** | 0.24*** | ns | 0.44*** | 0.71*** | ns | 1.00 | |
| C/SS | 0.05* | ns | ns | 0.17*** | 0.13*** | 0.12** | 0.08** | ns | 0.22*** | 0.11** | **−0.55*** | 0.09** | 1.00 |

Table 2. Spatial variability of the investigated physical and chemical parameters: samples were classed as surface samples ($n = 25$), samples collected at 1 m and 3 m layers ($n = 26$) and samples collected at deeper layers ($<3$ m) samples ($n = 24$). The mean for the total samples ($n = 75$) is also indicated. ANOVA was performed to assess the significance of quantitiative differences along the water column for each variable. H and L: significantly higher and lower, respectively; ANOVA, ns: not significant, *: $P < 0.05$, **: $P < 0.01$, ***: $P < 0.001$.

| Parameter | Temp. (°C) | Salin. | D.O. (mg l⁻¹) | NH₄⁺ (μM) | NO₃⁻-NO₂⁻ (μM) | PO₄³⁻ (μM) | Si(OH)₄ (μM) | Chl a (μg l⁻¹) | Pheop. (μg l⁻¹) | POC (μg l⁻¹) | SS (mg l⁻¹) | C/Chl a (ratio) | C/SS (mg g⁻¹) |
|---|---|---|---|---|---|---|---|---|---|---|---|---|---|
| Surface ($n = 25$) | | | | | | | | | | | | | |
| AVG | 18.3 | 27.1 | 7.8 | 23.2 | 23.9 | 2.82 | 35.5 | 1.8 | 1.6 | 811.4 | 21.0 | 460.0 | 51.0 |
| SD | 1.3 | 4.3 | 1.0 | 11.0 | 14.6 | 1.26 | 19.7 | 0.4 | 1.1 | 318.9 | 14.1 | 177.9 | 24.7 |
| 1–3 m ($n = 26$) | | | | | | | | | | | | | |
| AVG | 16.9 | 31.8 | 8.2 | 10.8 | 8.4 | 1.46 | 16.0 | 1.6 | 1.0 | 535.0 | 18.8 | 338.7 | 40.2 |
| SD | 0.5 | 0.2 | 0.4 | 4.7 | 4.1 | 0.61 | 5.4 | 0.3 | 1.0 | 218.3 | 13.5 | 136.0 | 19.3 |
| <3 m ($n = 24$) | | | | | | | | | | | | | |
| AVG | 16.5 | 32.0 | 8.0 | 8.1 | 4.7 | 1.19 | 12.0 | 1.6 | 1.1 | 516.4 | 19.6 | 317.2 | 34.1 |
| SD | 0.1 | 0.0 | 0.3 | 2.9 | 1.8 | 0.43 | 3.0 | 0.4 | 1.0 | 260.9 | 13.0 | 116.1 | 14.8 |
| Total ($n = 75$) | | | | | | | | | | | | | |
| AVG | 17.2 | 30.3 | 8.0 | 14.1 | 12.4 | 1.83 | 21.2 | 1.7 | 1.2 | 621.2 | 19.8 | 372.3 | 41.8 |
| SD | 1.1 | 3.3 | 0.7 | 9.7 | 12.1 | 1.10 | 15.7 | 0.4 | 1.0 | 297.7 | 13.4 | 157.1 | 21.0 |
| ANOVA | | | | | | | | | | | | | |
| surf. vs. 1–3 m | H*** | L*** | L* | H*** | H*** | H*** | H*** | ns | ns | H** | ns | H* | ns |
| surf. vs. <3 m | H*** | L*** | ns | H*** | H*** | H*** | H*** | ns | ns | H*** | ns | H*** | H** |
| 1–3 m vs. <3 m | H*** | L*** | ns | H* | H*** | ns | H** | ns | ns | ns | ns | ns | ns |

Table 3. Temporal variability of the investigated physical and chemical parameters. According to the tidal level prediceted by the Maritime Safety Agency, Takamatsu, the time series was divided into an ebbing period (14:00–19:00 and 2:00–8:00, $n = 39$) and a flood period (10:00–13:00, 20:00–01:00 and 9:00–10:00, $n = 36$). The mean during both ebb and flood periods and the ratio between ebb and flood values (ebb/flood) are given for each variable. ANOVA was performed to assess the significance of differences between ebb and flood values, ns: not significant, *: $P < 0.05$, **: $P < 0.01$, ***: $P < 0.001$.

| Parameter | Unit | Flood | Ebb | Ebb/Flood | ANOVA |
|---|---|---|---|---|---|
| Temp. | °C | 17.1 ± 0.8 | 17.4 ± 1.4 | 1.02 | ns |
| Salin. | | 30.6 ± 3.1 | 30.0 ± 3.6 | 0.98 | ns |
| D.O. | mg l$^{-1}$ | 8.2 ± 0.7 | 7.8 ± 0.6 | 0.95 | * |
| $NH_4^+$ | $\mu$M | 10.6 ± 8.1 | 17.3 ± 9.9 | 1.64 | ** |
| $NO_3^--NO_2^-$ | $\mu$M | 8.7 ± 9.8 | 15.8 ± 13.1 | 1.81 | ** |
| $PO_4^{3-}$ | $\mu$M | 1.4 ± 1.0 | 2.2 ± 1.1 | 1.56 | ** |
| $Si(OH)_4$ | $\mu$M | 17.0 ± 13.9 | 25.1 ± 16.3 | 1.47 | * |
| Chl $a$ | $\mu$g l$^{-1}$ | 1.7 ± 0.4 | 1.6 ± 0.4 | 0.93 | ns |
| Pheop. | $\mu$g l$^{-1}$ | 0.6 ± 0.5 | 1.8 ± 1.0 | 3.05 | *** |
| POC | $\mu$g l$^{-1}$ | 473 ± 231 | 758 ± 289 | 1.60 | *** |
| SS | mg l$^{-1}$ | 23.5 ± 16.9 | 16.4 ± 7.8 | 0.70 | * |
| C/Chl $a$ | ratio | 274 ± 129 | 463 ± 123 | 1.69 | *** |
| C/SS | mg g$^{-1}$ | 33.5 ± 21.1 | 49.5 ± 17.9 | 1.48 | *** |

## 3.5 Spatial variability: differences between layers

To assess and quantify spatial differences through the water column, we divided our sample data-set according to three different layers: the surface ($n = 25$), the intermediate layer including all samples at 1 m and 3 m ($n = 26$), and the lower layer, including all samples below 3 m ($n = 24$) (Table 2).

Temperature and salinity were significantly higher and lower ($P < 0.001$), respectively, at the surface (mean: 18.3 ± 1.3°C and 27.1 ± 4.3) than in both the intermediate and the lower layer (Table 2). Highly significant differences ($P < 0.001$) also occurred between the intermediate layer and the lower layer, the latter displaying the lowest temperature and the highest salinity values (mean: 16.5 ± 0.1°C and 32.0 ± 0.0). In contrast, D.O. concentration was only lower at the surface than in the intermediate layer, albeit with a lesser degree of significance ($P < 0.05$). Among the investigated physical and chemical parameters, nutrient concentrations showed the strongest quantitative differences among all layers (Table 2). They were highest at the surface, with mean values of 23.2 ± 11.0 $\mu$M (ammonium), 23.9 ± 14.6 $\mu$M (nitrate + nitrite), 2.82 ± 1.26 $\mu$M (phosphate) and 35.5 ± 19.7 $\mu$M (silicate), and lowest at the lower layer (Table 2). Accordingly, nutrient concentrations were 1.9 (phosphate) to 2.8 (nitrate + nitrite) times and 2.4 (phosphate) to 5.1 (nitrate + nitrite) times higher at the surface than at the intermediate and the lower layer, respectively, all of these differences being highly significant ($P < 0.001$). Differences were less marked between the intermediate and the lower layer, varying from highly significant (nitrate + nitrite) to not significant (phosphate). Among SPM, the

POC content was significantly higher at the surface than in both the intermediate ($P < 0.01$) and the lower ($P < 0.001$) layer. However, the extent of quantitative differences between layers was more restricted than that found for nutrients and was within the same order of magnitude (Table 2). Furthermore, both Chl $a$ and pheopigments showed no significant differences between layers. The C/Chl $a$ and C/SS ratios were also within the same order of magnitude, being significantly higher at the surface than at the lower layers, while not significantly different between the intermediate and the lower layer.

## 3.6 Temporal variability: ebb versus flood

As a further step in investigating the effect of a tidal cycle on the variability of physical and chemical water parameters, we divided our samples, according to the predicted tidal levels (Maritime Safety Agency, Takamatsu), into two data-sets representing an ebb situation and a flood situation. The ebb situation included samples collected between 14:00 and 19:00 and between 2:00 and 8:00 ($n = 39$) and the flood situation included samples collected between 10:00 and 13:00, 20:00 and 1:00 and 9:00 and 10:00 ($n = 36$). Table 3 shows that pheopigments, POC and all nutrient species concentrations were significantly higher during the ebb. In contrast, both temperature and salinity, the major variability of which was restricted to the uppermost 2–3 m or the surface, respectively (Figs. 2(a) and (b)), were not significantly different between an ebb and a flood situation. It is interesting to note that while nutrient concentrations showed a much greater difference between layers than SPM (Table 2), most SPM components had a more marked and significant difference on a

temporal basis (Table 3). Most remarkably, the pheopigment content was 3.1 times higher during the ebb (1.8 ± 1.0 $\mu$g l$^{-1}$) than during the flood (0.6 ± 0.5 $\mu$g l$^{-1}$) (Table 3). According to the different extent of ebb vs. flood change of Chl $a$ and pheopigments, the pheopigment/Chl $a$ ratio also increased 3.1 times ($P < 0.001$, data not shown) during the ebb.

## 4. Discussion

### 4.1 Temperature, salinity and dissolved oxygen concentration

Change of temperature was strongly related to both the river runoff during the ebb flow, which had a higher temperature than sea water (Montani et al., 1998), and heat transfer through the sea surface during the day. Accordingly, these two processes caused a major increase of temperature at the uppermost 2–3 m layers during the lower low tide, which occurred in the afternoon of May 30 (Fig. 2(a)). A low-salinity surface water mass moving down-estuary with the ebb led to stratification between the surface and the subsurface layers. The effect of fresh water intrusion into the subtidal zone was strongest between the lower low tide and the higher high tide (Fig. 2(b)). During the second ebb, the variation of both temperature and salinity was more restricted. This coincided with a higher tidal level (+105 cm) than had occurred on the previous day (+35 cm). Our results are consonant with the study by Uncles and Stephens (1996), who showed that salinity intrusion was a strong function of spring-neap tidal state and a weaker function of fresh water inflow; they also give additional information on the within-one-tidal-cycle behaviour of salt intrusion.

Although D.O. showed no significant correlation with either temperature or salinity (Table 1), a relative decrease of D.O. concentration in surface water coincided with an increase of temperature (Fig. 2(a)) and a decrease of salinity (Fig. 2(b)) during both low tides (Fig. 2(c)). Accordingly, D.O. correlated negatively with all nutrient species and several components of SPM, although to a lesser extent than salinity (Table 1). This was an indication that relatively lower D.O. water mass was brought into the subtidal zone from the inner part of the estuary. In a parallel survey conducted simultaneously during the present time series we found that D.O. concentration was indeed lower at an intermediate intertidal site (i.e. lowest D.O. values averaging 2.5 ± 0.5 mg l$^{-1}$ between 5:00 and 9:00, with a 24-h mean of 5.2 ± 1.6 mg l$^{-1}$) than at Stn. Y3 (Montani et al., 1998). D.O. concentration also tended to decrease in the lower layers of the water column, down to the bottom, at night and through the whole water column before the sunrise. We can relate this to a temporary tendency of respiration processes to over whelm primary production processes in the absence of light. This was

also indicated by an overall decrease of the Chl $a$ content <1.5 $\mu$g l$^{-1}$ between 24:00 and 6:00 (Fig. 4(a)). A normoxic condition remained during the entire period of this survey, however.

### 4.2 Spatial and temporal variability of nutrients and their origin

The greatest change of nutrient concentrations occurred at the surface, up to an increase of 8.9 times for ammonium (from 4.8 $\mu$M to 42.6 $\mu$M, between 23:00 and 3:00), 11.2 times for nitrate + nitrite (from 4.5 $\mu$M to 50.3 $\mu$M, between 23:00 and 2:00), 8.6 times for phosphate (from 0.57 $\mu$M to 4.9 $\mu$M, between 11:00 and 20:00) and 8.0 times for silicate (from 9.6 $\mu$M to 76.7 $\mu$M, between 11:00 and 20:00) (Figs. 3(a), (b), (c) and (d)). The spatial variability in nutrient concentrations through the water column was consistent over the complete time series, with highly significant ($P < 0.001$) differences between the surface and the subsurface layers (Table 2). The present study also demonstrates that major changes in nutrient concentrations occur temporally, depending on the tides, which were quantified to be nitrate + nitrite concentration up to 1.8 times higher during the ebb than during the flood (Table 3). In contrast, a larger tidal amplitude (i.e. between the lower low tide and the higher high tide) did not cause a much stronger increase of nutrient concentrations through the water column, while it was more evident at the surface, particularly in the inner part of the estuary (Montani et al., 1998). Nevertheless, the highly significant ($P < 0.001$) negative correlation of nutrients with salinity (Table 1) was direct evidence that a low salinity water mass with high nutrient concentrations was brought into the subtidal zone from the inner part of the estuary. In our associated work (Montani et al., 1998) we observed a contrasting behaviour of the different nutrient species. In particular, we found that the fresh water runoff was a major source of silicate and nitrate + nitrite, the concentrations of which correlated highly negatively with salinity, most significantly at an upper riverine station ($R^2 = 0.88$ and $R^2 = 0.80$, respectively, $P < 0.001$, Montani et al., 1998). In contrast, ammonium and phosphate were found to be added at intermediate salinity values at inner intertidal sites. At the same time, the latter nutrient species correlated significantly with salinity at Stn. Y3, as this station was less affected by low salinity water mass intrusion along the transect line surveyed (Montani et al., 1998). It can be noted that in the present study the correlation of ammonium and phosphate with salinity also had relatively lower $R^2$ values than silicate and nitrate + nitrite (Table 1). In addition, the stronger (negative) correlation of ammonium and phosphate with D.O. (Table 1) also demonstrated that ammonium and phosphate had a move intertidal origin than silicate and nitrate + nitrite. For the former two species of nutrients,

we previously highlighted a major addition at intermediate salinity, also on a seasonal basis (Magni and Montani, 2000). This relates to the important effect of processes of benthic nutrient regeneration within the estuary, particularly in the intertidal zone due to the excretory activity of macrofauna (Magni *et al.*, 2000b). The results of the present study further clarify the spatial and temporal extent to which nutrients are exported into the subtidal zone as a result of the tidal cycle, confirming their riverine and/or intertidal origin.

### 4.3 Variability of SPM compounds and tidally-mediated particle selection transport

As for all nutrient species, pheopigments and POC (Figs. 4(b) and (c), respectively) increased strongly due to the effect of the tidal cycle, as they were transported from the inner part of the estuary into the subtidal zone. This was most remarkable on May 30, between the lower low tide (e.g. 16:00, the water column) and the higher high tide (e.g. from 20:00 and 23:00, the surface), viz., during the period of largest tidal amplitude. Accordingly, these two SPM components were highly correlated with each other ($R^2 = 0.62$, $P < 0.001$; Table 1). In contrast, Chl *a* had a much more limited range of spatial and temporal variability (Fig. 2(a)) and its correlation with both pheopigments and POC was, although significant, much weaker ($R^2 = 0.12$ and $R^2 = 0.17$, respectively, Table 1). We also observed similar correlations between POC and phytopigments on a seasonal basis, during a 2-year period survey conducted at a creek crossing the adjacent intertidal flat during low tide (Magni and Montani, 2000). We found that the Chl *a* content in ebbing water was on average *ca.* 3 times lower than the pheopigment content and, similarly to the present study, it showed a more restricted range of variability. This relates to the presence of a large fraction of refractory algal materials, rather than living phyto-carbon (*ca.* 5%), on the adjacent intertidal flat (Magni and Montani, 1998, 2000). The present work supports our previous findings, clearly showing that a considerable amount of algal derived organic carbon of intertidal origin is transported into the subtidal zone due the effect of a tidal cycle and amplitude.

The C/Chl *a* ratio (Fig. 4(e)) showed a spatial and temporal variability similar to that of pheopigments (Fig. 4(b)) and POC (Fig. 4(c)). Our C/Chl *a* ratio, up to 500–600 and exceptionally 800 (Fig. 4(e)), was lower than that indicated in Lake Pontchrtrain (Gulf of Mexico) (Bianchi and Argyrou, 1997). In Lake Pontchrtrain, the C/Chl *a* ratio was highest (1608 ± 942) when the Chl *a* concentration was at its lowest and the riverine discharge was at its highest. Bianchi and Argyrou (1997) found that 55% of the total Chl *a* was mostly derived from inputs of degraded vascular plant detritus. In our study area, a relatively lower C/Chl *a* ratio indicates that allochthonous sources (i.e.

wetland input of organic carbon, leading to an increase of the C/Chl *a* ratio) are not of primary relevance. In contrast, the strong correlation of the C/Chl *a* ratio with both pheopigments and POC and the absence of a significant correlation with Chl *a* (Table 1) further indicated that the intertidal zone is a major source of organic carbon to the subtidal zone.

In contrast to the distributional pattern of pheopigments (Fig. 4(b)) and POC (Fig. 4(c)), the SS content was relatively low during the ebb flow (14:00–19:00) and, by contrast, it increased sharply with the surging flood, during the higher high tide (Fig. 4(d)). SS did not correlate significantly with any nutrient species, nor any component of SPM (Table 1). However, a detailed examination of the spatial and temporal variability of SS and POC highlighted a differentiated particles transport characterized by a different organic content in relation to both depth and tidal state. To assess such differences, we used two major cut points, such as 35 mg l$^{-1}$ for SS and 1000 $\mu$g l$^{-1}$ for POC, and accordingly divided the sample data-set into four different compartments (Fig. 5). The sample points characterized by SS <35 mg l$^{-1}$ and POC <1000 $\mu$g l$^{-1}$ and those characterized by SS >35 mg l$^{-1}$ and POC >1000 $\mu$g l$^{-1}$ were included in a best-fit regression line which represented the major portion of the samples (72%, $n = 54$, Fig. 5). In contrast to no correlation between POC and SS on an all-sample basis (Table 1), the samples divided in this was showed a highly significant correlation, described by the equation SS = 0.028 × POC − 2.35, $R^2 = 0.64$, $P < 0.001$ (Fig. 5). This subdivision also enabled us to describe major changes occurred during the time series. At the start of the survey, from 10:00 to 12:00, both POC and SS concentration were low (sampling points given by a circled letter *a*, Fig. 5). In contrast, within the next few hours, during the ebb, the SS concentration remained <35 mg l$^{-1}$ (Fig. 4(d)), while the POC content increased markedly, particularly at 16:00 (Fig. 4(c)), up to >1000 $\mu$g l$^{-1}$. As a result, these organically-richer samples (sampling points given by a circled letter *b*, Fig. 5) deviated from the regression line. Nevertheless, the C/SS ratio did not change significantly from the previous hours, most values being rather high at >40 mg g$^{-1}$ (Fig. 4(f)). Subsequently, between 19:00 and 24:00, before the highest level of the higher high tide was reached (0:24), the SS content increased sharply through the water column to >35 mg l$^{-1}$, while the POC content decreased markedly below the surface. This corresponded to a strong decrease of the C/SS ratio, indicating that organically-poorer samples were being transported into the subtidal site. In addition, these samples could be further split according to the POC cut point (1000 $\mu$g l$^{-1}$). Interestingly, only surface samples were found to have a parallel POC content >1000 $\mu$g l$^{-1}$ (sampling points given as circled letters *c1*, Fig. 5). In contrast, most samples be-
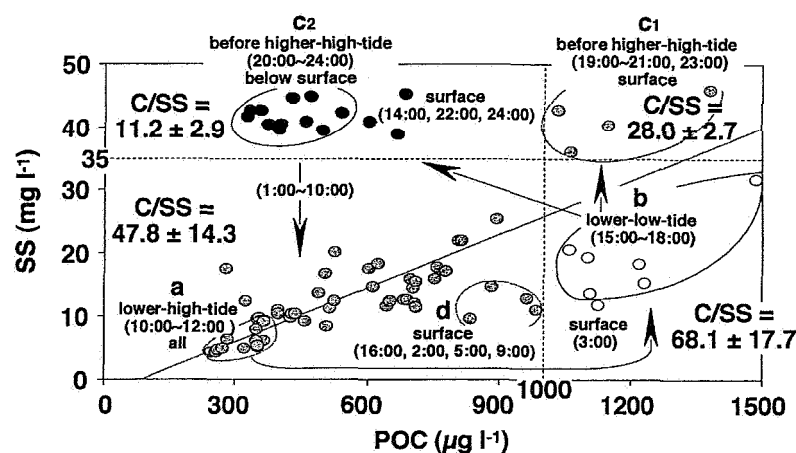
Fig. 5. Plots of suspended solid (SS) against particulate organic carbon (POC). The regression analysis for all SS (Fig. 4(d)) and POC (Fig. 4(c)) samples ($n = 75$) showed no significant correlation (Table 1). Samples were subsequently split in order to evaluate any inconsistency and to investigate the spatial and temporal variability of these two parameters. Two cut points were used, such as 35 mg $l^{-1}$ for SS and 1000 $\mu g$ $l^{-1}$ for POC, which accordingly divided the sample data-set into four different compartments. A best-fit linear regression line was constructed which highlighted a highly significant positive correlation for most samples (i.e. all sample points in grey: SS $= 0.028 \times$ POC $- 2.35$, $R^2 = 0.64$, $P < 0.001$, $n = 54$). This excluded "relatively lighter (SS $<35$ mg $l^{-1}$)—very organically rich (POC $>1000$ $\mu g$ $l^{-1}$)" samples (sample points in white, $n = 11$) and "heavier (SS $>35$ mg $l^{-1}$)—relatively non-organically rich (POC $<1000$ $\mu g$ $l^{-1}$)" samples (sample points in black, $n = 14$). Letters in this figure indicate: (a) all samples from 10:00 to 12:00 ($n = 12$); (b) surface from 15:00 to 18:00 and 1-3-7 m at 16:00 ($n = 7$); (c1) surface from 19:00 to 21:00 and at 23:00 ($n = 4$); (c2) all layers below the surface from 20:00 to 24:00, but 5 m at 22:00 ($n = 11$); (d) surface at 16:00, 2:00, 5:00 and 9:00 ($n = 4$); non-circled-sample points in black: surface at 14:00, 22:00 and 24:00 ($n = 3$). The mean C/SS ratio (mg $g^{-1}$) is also indicated for each of the four compartments.

low the POC cut point, yet with a SS content $>35$ mg $l^{-1}$, were those below the surface (sampling points given as circled letters $c2$, Fig. 5). All samples characterized by SS $>35$ mg $l^{-1}$ and POC $<1000$ $\mu g$ $l^{-1}$ had the lowest C/SS ratio values, as they were the organically-poorest ones, and accordingly deviated strongly from the linear regression line (Fig. 5). Most of the remaining samples collected during the time series were those collected between 1:00 and 10:00, which represented the core data-set forming the regression line. Again, some surface samples could be characterized by a relatively high POC content and a relatively low SS content (sampling points given as letter $d$, Fig. 5). This pattern indicates that particle selection occurs not only temporally, as related to the tidal state and amplitude, but also spatially through the water column, as organically-richer particles tend to be transported through the surface, the most affected layer by intrusion of a low-salinity (Fig. 2(b)) and high-nutrient (Figs. 4(a), (b), (c) and (d)) water mass. Overall, these results demonstrate that lighter suspended particles (with a higher pheopigment and POC content, and a low SS content) are transported from the intertidal zone into the subtidal zone while decreasing the tidal level. Conversely, a greater fraction of SS is exported during the subsequent surging flood. This implies that a major process affecting the water chemistry of the subtidal site includes

resuspension and transport of fine particles from the adjacent intertidal flat, characterized by surface sediments with a lower organic carbon content (TOC $= 10.3 \pm 8.6$ mg $g^{-1}$; Magni and Montani, 1998) than is found in SPM (Fig. 4(f)). Thus, heavier SPM corresponded to a decrease of the C/SS content due to an increase of organically-poorer sediment particles. As related to the effect of the tidal amplitude, sediment resuspension and the decrease of the C/SS content in our samples was strongest after the lower low tide ($+35$ cm at 17:28). This was enhanced by the exposure of the intertidal flat, which occurs at a tidal level of $ca.$ 50 cm (Magni and Montani, 1998). Finally, temporal variations were stronger during the lower low tide ($+35$ cm) than during the higher low tide ($+105$ cm), confirming the importance of the tidal amplitude on the transport of particulate compounds into the subtidal zone.

On a seasonal and annual basis, we found that pheopigment and POC concentrations were much higher in ebbing water than at the surface of Stn. Y3, while nutrient concentrations were within the same order of magnitude (Magni and Montani, 2000). We suggested that such a qualitative difference (i.e. nutrients vs. SPM) between sites can be related to particle deposition and/or removal along the estuary, resulting in a limited SPM concentration at the surface layer of the subtidal site, while

nutrients are more directly transported into the surface layer of the subtidal zone by lower salinity water mass intrusion from the intertidal zone. The different spatial distribution through the water column between SPM and nutrients presented in this study are a direct evidence of our original hypothesis. The results also have important ecological implications. We infer that the daily export of particulate compounds through the water column represents a major source of carbon to the bottom sediments at Stn. Y3, likely vulnerable to an excessive organic load from the inner part of the estuary. We do indeed observe a seasonal mortality of macrofauna at this station due to an increase of organic load, leading to the enhancement of anaerobic decomposition and oxygen depletion in sediments between late summer and early autumn both in 1994 and 1995 (Magni and Montani, 1998).

## References

Balls, P. W. (1992): Nutrient behaviour in two contrasting Scottish estuaries, the Forth and the Tay. *Oceanol. Acta*, **15**, 261–277.

Balls, P. W. (1994): Nutrient inputs to estuaries from nine Scottish east coast rivers; influence of estuarine processes on inputs to the North Sea. *Estuar., Coast. Shelf Sci.*, **39**, 329–352.

Bennett, J. P., J. W. Woodward and D. J. Shultz (1986): Effect of discharge on the chlorophyll *a* distribution in the tidally-influenced Potamoc river. *Estuaries*, **9**, 250–260.

Bianchi, T. S. and M. E. Argyrou (1997): Temporal and spatial dynamics of particulate organic carbon in the lake Pontchartrain estuary, Southern Louisiana, U.S.A. *Estuar., Coast. Shelf Sci.*, **45**, 557–569.

Caffrey, J. N. and J. W. Day, Jr. (1986): Control of the variability of nutrients and suspended sediments in a Gulf coast estuary by climatic forcing and spring discharge of the Atchafalaya river. *Estuaries*, **9**, 295–300.

Clark, J. F., H. J. Simpson, R. F. Bopp and B. Deck (1992): Geochemistry and loading history of phosphate and silicate in the Hudson estuary. *Estuar., Coast. Shelf Sci.*, **34**, 213–233.

Cowan, J. L. W., J. R. Pennock and W. R. Boyton (1996): Seasonal and interannual pattern of sediment-water nutrient fluxes in Mobile Bay, Alabama (USA): regulating factors and ecological significance. *Mar. Ecol. Prog. Ser.*, **141**, 229–245.

De Madariaga, I. (1995): Photosynthetic characteristics of phytoplankton during the development of a summer bloom in the Urdaibai estuary, Bay of Biscay. *Estuar., Coast. Shelf Sci.*, **40**, 559–575.

Dyer, K. R., M. C. Christie, N. Feates, M. J. Fennessy, M. Pejrup and W. van der Lee (2000): An investigation into processes influencing the morphodynamics of an intertidal mudflat, the Dollard estuary, The Netherlands: I. Hydrodynamics and suspended sediments. *Estuar., Coast. Shelf Sci.*, **50**, 607–625.

Eyre, B. and C. Twigg (1997): Nutrient behaviour during post-flood recovery of the Richmond river estuary northern NSW, Australia. *Estuar., Coast. Shelf Sci.*, **44**, 311–326.

Hernandez-Ayon, J. M., M. S. Galindo-Bect, B. P. Flores-Baez and S. Alvarez-Borrego (1993): Nutrient concentrations are high in the turbid waters of the Colorado river Delta. *Estuar., Coast. Shelf Sci.*, **37**, 593–602.

Lorenzen, C. J. (1967): Determination of chlorophyll and pheopigments: spectrophotometric equations. *Limnol. Oceanogr.*, **12**, 343–346.

Magni, P. (1998): A multidisciplinary study on the dynamics of biophilic elements (C, N, P, Si) in a tidal estuary of the Seto Inland Sea, Japan: physico-chemical variability and macrozoobenthic communities. Ph.D. Thesis, The United Graduate School of Ehime University, Japan, 258 pp.

Magni, P. and S. Montani (1997): Development of benthic microalgal assemblages on an intertidal flat in the Seto Inland Sea, Japan: effects of environmental variability. *La mer*, **35**, 137–148.

Magni, P. and S. Montani (1998): Responses of intertidal and subtidal communities of the macrobenthos to organic load and oxygen depletion in the Seto Inland Sea, Japan. *Journal de Recherche Océanographique*, **23**, 47–56.

Magni, P. and S. Montani (2000): Water chemistry variability in the lower intertidal zone of an estuary in the Seto Inland Sea, Japan: seasonal patterns of nutrients and particulate compounds. *Hydrobiologia*, **432**, 9–23.

Magni, P., N. Abe and S. Montani (2000a): Quantification of microphytobenthos biomass in intertidal sediments: layer-dependent variation of chlorophyll *a* content determined by spectrophotometric and HPLC methods. *La mer*, **38**, 57–63.

Magni, P., S. Montani, C. Takada and H. Tsutsumi (2000b): Temporal scaling and relevance of bivalve nutrient excretion on a tidal flat of the Seto Inland Sea, Japan. *Mar. Ecol. Prog. Ser.*, **198**, 139–155.

Montani, S., P. Magni, M. Shimamoto, N. Abe and K. Okutani (1998): The effect of a tidal cycle on the dynamics of nutrients in a tidal estuary in the Seto Inland Sea, Japan. *J. Oceanogr.*, **54**, 65–76.

Murakami, T., C. Isaji, N. Kuroda, K. Yoshida and H. Haga (1992): Potamoplanktonic diatoms in the Nagara river; flora, population dynamics and influences on water quality. *Japan. J. Limnol.*, **53**, 1–12.

Murakami, T., C. Isaji, N. Kuroda, K. Yoshida, H. Haga, Y. Watanabe and Y. Saijo (1994): Development of potamoplanktonic diatoms in downreaches of Japanese rivers. *Japan. J. Limnol.*, **55**, 13–21.

Page, H. M., R. L. Petty and D. E. Meade (1995): Influence of watershed runoff on nutrient dynamics in a southern California salt marsh. *Estuar., Coast. Shelf Sci.*, **41**, 163–180.

Parsons, T. R., M. Maita and C. M. Lalli (1984): A *Manual of Chemical and Biological Methods for Seawater Analysis*. Pergamon Press, Oxford, 173 pp.

Renshun, Z. (1992): Suspended sediment transport processes on tidal mud flat in Jiangsu Province, China. *Estuar., Coast. Shelf Sci.*, **35**, 225–233.

Schubel, R. J. and D. W. Pritchard (1986): Responses of upper Chesapeake Bay to variations in discharge of the Susquehanna river. *Estuaries*, **9**, 236–249.

Sokal, R. R. and F. J. Rohlf (1995): *Biometry*. Freeman & Company, New York, 887 pp.

Strickland, J. D. H. and T. R. Parsons (1972): *A Practical Handbook of Seawater Analysis. Fisheries Research Board of Canada Bulletin*, **167**, 310 pp.

Uncles, R. J. and J. A. Stephens (1996): Salt intrusion in the Tweed Estuary. *Estuar., Coast. Shelf Sci.*, **43**, 271–293.

Vörösmarty, C. J. and T. C. Loder, III (1994): Spring-neap tidal contrasts and nutrient dynamics in a marsh-dominated estuary. *Estuaries*, **17**, 537–551.

Ward, L. G. and R. R. Twilley (1986): Seasonal distributions of suspended particulate material and dissolved nutrients in a coastal plain estuary. *Estuaries*, **9**, 156–168.

Yin, K., P. J. Harrison, S. Pond and R. J. Beamish (1995a): Entrainment of nitrate in the Fraser river estuary and its biological implications. I. Effects of salt wedge. *Estuar., Coast. Shelf Sci.*, **40**, 505–528.

Yin, K., P. J. Harrison, S. Pond and R. J. Beamish (1995b): Entrainment of nitrate in the Fraser river estuary and its biological implications. II. Effects of spring vs. neap tide and river discharge. *Estuar., Coast. Shelf Sci.*, **40**, 529–544.

Yin, K., P. J. Harrison, S. Pond and R. J. Beamish (1995c): Entrainment of nitrate in the Fraser river estuary and its biological implications. III. Effects of winds. *Estuar., Coast. Shelf Sci.*, **40**, 545–558.